KTH Royal Institute of Technology
Department of Mechatronics

Spring Term Report MF2121
The Rapid ZD-Tester 2.0

Astrid Bäckström, Arvid Hjort, Carl Bermhed, Erik Gelfgren,
Haoran Guo, Hataipat Sirirattanaphan, Matteo Tirillò, Oscar Held

Course Coordinator: Björn Möller

May 22, 2025

Abstract

In this report, the research and design process is presented for the development of a new Rapid ZD-Tester for RISE. Despite its current inoperable state, the existing testing machine was chosen as a foundational basis for the project based on time and budget constraints.

Based on stakeholder requirements and the allocated budget, a two-sensor solution, incorporating a vacuum clamping technique to ensure secure sample handling during testing, was selected. A state-of-the-art analysis was conducted to explore how similar challenges have been addressed in industrial applications and academic research, eventually identifying linear encoders and piezoelectric force sensors as the most suitable options for the objectives.

Consequently, a comprehensive design concept was developed, integrating these technologies along with the necessary hardware for signal processing. The final design concept includes the implementation of sensors directly attached to the machine's probe and the utilization of air supply available at the RISE labs for the vacuum system.

Future planning was also conducted focusing on analysing organizational challenges and planning for the Autumn semester while maintaining active communication with suppliers to procure the required hardware components.

Acknowledgements

We would like to thank Cecilia Rydfalk and Hans Christiansson for providing guidance in this project as well as the coaching team at KTH for their valuable feedback and helpful insights.

We would also like to acknowledge the use of Open AI's ChatGPT for the purpose of checking grammar within the report as well as to find relevant research articles.

Contents

1 Introduction **5**
1.1 Background . . . 5
1.2 Problem Statement . . . 5
1.3 Scope . . . 5
1.4 Stakeholders . . . 6
1.5 Organization . . . 6
1.6 Requirements . . . 7

2 State of The Art **8**
2.1 Old ZD-Tester . . . 8
2.1.1 Key Mechanical Principles and Measurement Methods . . . 8
2.2 Dynamic Decoupling of the Probe . . . 9
2.2.1 Limitations . . . 10
2.3 Displacement Sensors . . . 10
2.3.1 Linear Variable Differential Transformer . . . 11
2.3.2 Linear Encoders . . . 11
2.3.3 Eddy Current Sensors . . . 12
2.3.4 Laser Sensors . . . 12
2.4 Force and Acceleration Sensors . . . 12
2.4.1 Accelerometers . . . 13
2.4.2 Piezoelectric Force Sensors . . . 13
2.4.3 Strain Gauges Cells . . . 13
2.5 Thickness Calibration . . . 14
2.5.1 Standards for Thickness Measurements . . . 14
2.5.2 Electrical-Torque Algorithm . . . 14
2.6 Securing the Sample . . . 14
2.6.1 Vacuum Clamping . . . 14
2.6.2 Electrostatic Chuck . . . 15
2.6.3 Adhesive Fixation . . . 15
2.6.4 Mechanical Clamping . . . 15
2.7 Sampling . . . 15
2.7.1 DAQ . . . 15
2.7.2 Custom Solutions . . . 16

3 Design Concept **17**
3.1 General Concept . . . 17
3.2 Implementation of sensor system . . . 18
3.3 Impulse Generation . . . 19
3.4 Vacuum Clamping System . . . 19

4 Discussion **21**
4.1 Challenges for the Autumn Semester . . . 21
4.2 Future Work . . . 21

A Autumn Plan **26**

B Risk Assessment **28**

List of Figures

1 Probe Decoupling 10
2 Example of LVDT from top to bottom: Solenoid coils, Armature and Cylindrical tube [1] 11
3 Three concepts for the new machine 17
4 The final concept of the system 18
5 The concept diagram of a vacuum clamping system 20
6 GANTT Chart for Phase 2 26
7 GANTT Chart for Phase 3 27
8 Risk Assessment Report (RISE) 28

1 Introduction

This section outlines the background, problem, scope, organization, stakeholder, and requirements of the project.

1.1 Background

The growing environmental concerns surrounding packaging materials are increasing the focus on cellulose-based materials, such as paper and paperboard [2]. Paper and paperboard-based materials are among the most widely used packaging forms for food products, including beverages, milk, and other dairy products [3].

The mechanical properties of paperboard are essential for large-scale industrial processes such as flexographic printing; which works by means of high-speed rollers that briefly compress the material in milliseconds, making the materials response to rapid compression critical for printing quality. During printing, the paperboard is subjected to compressive forces perpendicular to their surface in order to transfer the graphics. Flexographic printing is the most commonly used method among the printing techniques for paperboard materials [4]. Flexographic printing is a high-speed process where plates made out of flexible photopolymer transfers ink to a material. The plates are mounted onto a rotating cylinder that presses ink onto the material with the help of an impression cylinder and the method relies heavily on precise controlled pressure [5].

Measuring compressive properties in the thickness direction of these materials is difficult, but essential to understand their behaviour during printing. Typically, industry processes that convert paper operate at speeds nearly 1000 times faster than standard material testing rates. Since fibre-based materials are rate sensitive, testing must be performed at relevant speeds to accurately reflect their behaviour during conversion [6].

The project is part of a HK-Capstone Course at KTH and is for the Research Institutes of Sweden (RISE) who provided a measurement machine that could determine the viscoelastic properties of thin sheet materials such as paper and board products. The machine measures the initial thickness of the material and through application of a rapid compression produces a displacement-stress curve based on the material deformation during the impulse. It tests multiple points to produce a heat-map of the material.

1.2 Problem Statement

To measure the rapid compression property that is experienced in flexographic printing, RISE has previously used a machine called Rapid ZD-Tester. However, this machine is currently broken and is not able to satisfy RISE's requirements. Therefore, they need a new machine capable of providing the same measurements.

1.3 Scope

The aim of this project is to design, develop, and test a device for accurately measuring the deformation and thickness of paper and paperboard-like materials under dynamic impulse compression. The requirements are defined by our stakeholders, who expect the machine to deliver reliable measurements of the deformation, the applied pressure, and the thickness of the material. In addition, the requirements are adjusted by the participants, based on their capabilities and resources for carrying out the project. Therefore, the scope has been limited to only a few sub-functions of the entire machine. The sub-functions that will be worked on are:

- **Measure displacement:** Measure how much the paper deforms under the load.
- **Measure acceleration/force:** To determine the amount of force and acceleration applied during the impact.
- **Apply a rapid compression pulse:** A small probe is released from a controlled height to simulate the mechanical stress occurring in real-world applications of high-speed flexographic printing.
- **Calibrate initial thickness:** Before testing, the system must determine the initial thickness of the paper, so to adjust the measurement procedure accordingly.
- **Securing paper during measurement:** To ensure accurate results, the paper must remain fixed and flat during the test, without being damaged by the securing mechanism.

The sub-functions that will be excluded are:

- **Positioning of paper:** Consistent positioning of the probe ensures repeatable impact on the same location across samples, enabling reliable and comparable measurements.
- **Loading and unloading of test material:** A mechanism to automatically load and unload the paper into the machine when testing. After the test is completed, being able to unload the paper from the machine using the same mechanism.

The project also aims to enhance the participants' knowledge of mechatronics over the course of the project, which runs from March to December and includes a summer break.

1.4 Stakeholders

The stakeholders for this project is the Research Institute of Sweden, (RISE), is an independent, state-owned research and innovation partner with locations across Sweden. With nearly 3300 employees, RISE collaborates internationally with industry, academia, and the public sector to strengthen the competitiveness of Swedish businesses on a global scale. Through applied research, testing, and innovation services, RISE supports all types of innovation processes and contributes to building a sustainable society. The institute offers unique expertise and access to over 130 testbeds and demonstration environments dedicated to future-proof technologies, products, and services [7].

Our primary contact at RISE is researcher Cecilia Rydefalk. We also receive support from Hans Christiansson, who works as an application engineer at RISE.

1.5 Organization

This spring term the project was mainly focused on understanding the current Rapid ZD-Tester by identifying key challenges and requirements, and conducting research on sensor technology to support the future redesign. The team consisted of eight master students in the Mechatronics master program at KTH with a diverse collective background in mechatronics, mechanics and design.

Due to the research-oriented nature of this phase of the project, the team adopted a flexible organizational approach. Tasks were assigned based on the responsibilities associated with the state-of-the-art (SOTA), and on self-interest and experience, allowing team members to become knowledgeable about their respective topics. These included areas such as force impulse generation, sampling, sensors, and sample clamping.

Team coordination was maintained through regular meetings each week as well as bi-weekly meetings with the stakeholder. Shared documentation was achieved through Google Drive and Microsoft Teams. Code will later be shared using GitHub.

In the Autumn term, the organizational structure will change. Work will instead be based on identified sub-functions of the future machine. We acknowledge that this might not be the most efficient, but allows all team members to gain experience within major disciplines such as mechanical, electronics and control. Sub-teams will have regular internal meetings, in addition to cross-team communication to ensure system integration. As outlined in Appendix A, the team has developed a preliminary GANTT schedule to follow, together with a work breakdown structure (WBS), will serve as the main governing documents for coordination and task planning. During the weekly meetings, the whole team will be present to report progress through the GANTT. This structure is expected to support the team for the upcoming term.

1.6 Requirements

The requirements provided by the stakeholders are presented in Table 1. The table is divided into three columns: *Requirements, Technical requirements, and Flexibility.* The last column represents a rating on a scale from 1 to 5, where 1 indicates low flexibility and 5 indicates high flexibility. This parameter is crucial in determining the admissible slack for each requirement in the final product, ensuring a final solution that meets stakeholder expectations.

Requirements	Technical Requirements	Flexibility
Improve thickness range of measuring	Measuring boards from 100 µm to 1.5 mm	2
Reduce noise in the measurements	Less than 0.1 % of the measured signals amplitude	3
Have a high spatial resolution	Resolution of a minimum 0.5 µm in the Z direction	2
Probes shall be interchangeable	Possibility to use all the different sizes of probes and weights	2
Possible to sample high-rate deformation	Sample the position, acceleration/ force at 100 kHz	2
Adjustable probe height and release	Probe height should reach 160 µm above the test sample	1
Measurement process shall adapt to the local property of the sample point	Measure the thickness of the point before performing the measurement	1
Sample's properties shall be kept unchanged while testing	Machine only interacts with the sample material vertically	3
System shall generate a proper impulse force	Free impact on the surface capable of reaching 1 MPa pressure	1

Table 1: Requirements and Technical Requirements Table

2 State of The Art

Starting with a clear statement of the scope, outlined in Section 1.3, research was conducted to explore the current State-Of-The-Art for achieving objectives similar to those of interest in this project. To properly merge the information gathered from the current State-Of-The-Art into the final design concept, the requirements were carefully considered. The analysis begins with an overview of existing machines, followed by techniques for impulse generation, sensors, thickness calibration, paper clamping, and sampling.

2.1 Old ZD-Tester

The testing that RISE have been performing on print material have been completed by a process that is described in detail in the [8]. In summary it works by dropping a cylindrical probe and tracking its position to derive velocity and acceleration. This can then be used to produce a displacement-stress curve for the material over multiple coordinate positions of a single test piece, allowing for visualization in the form of a property mapping, highlighting the properties and inconsistencies of the material.

2.1.1 Key Mechanical Principles and Measurement Methods

To characterize these properties, RISE has used the Rapid ZD-tester. The device simulates millisecond-scale compression by a free-falling 200 g steel probe with a contact area of 5 mm in diameter. After having measured the local thickness of the impacting area, the probe is dropped at a height of 80 µm and left to bounce on the sample. The resulting average impact pressure is about 0.8 MPa, with a ∼1.5 ms impact duration. This is compared to the impact pressure of approximately 1 MPa of the flexographic nip. This is unlike the principle used in universal testing machines (UTMs), which apply a slow and controlled load. [8]

The measurement system is currently built around three key principles:

1. Dropping of the weighted probe - Generates fast compressive force by dropping a weight. The probe is allowed to bounce and record subsequent impacts. The force and impact velocity are dependent on the drop height and cannot be controlled independently. Using a free-falling mass eliminates the need for a force generating actuator which could introduce dynamical errors such as lag, damping and actuator overshoot.

2. Eddy-current displacement sensor - Is positioned under the sample and records the position of the probe.

3. Acceleration is numerically derived from displacement to calculate force, using Newton's second law. The double numerical differentiation increases noise into the final signal. This is particularly a problem for those parts of the force signal where rapid transitions occurs.

Each test location, before dropping the probe, undergoes a thickness measurement at 50 kPa to adjust the testing procedure. After this, the probe is released at each point twice, with 5 seconds in between drops, to ensure reliability by checking the measurement overlap. The tests are preformed over a 16 x 20 grid, resulting in 320 points, which provides a heat-map over the entire surface.

2.2 Dynamic Decoupling of the Probe

Due to the required precision of the measurement the inclusion of an actuator as the driving force would introduce unwanted dynamics. Due to this the probe was physically decoupled from the actuator in all but the negative z-direction. Meaning that the actuator could only move the probe in the out of plane direction. The decoupling used a double rod system as can be seen in figure 1, where the actuator could lift the probe at any pace. To initiate the impulse the actuator would then accelerate faster than 1 g as to decouple itself from the probe.

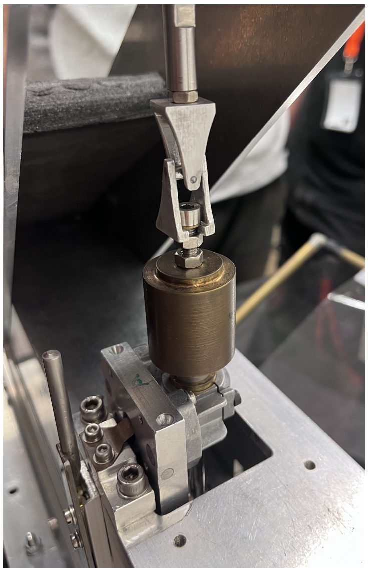

Figure 1: Probe Decoupling

2.2.1 Limitations

Although the Rapid ZD-tester offered valuable insight into the mechanical response of paperboard, several limitations were identified:

1. Indirect force measurement - The system did not directly measure the force, but instead derived the acceleration from displacement measurements and using the known weight calculated the force. This approach meant that switching probes was cumbersome and required a lot of setup and calibration. This also led to amplified signal noise and reduced accuracy, especially during transient events.

2. Semi-automatic test procedure - The clamping functionality used to secure the position of the paper during tests was manual and thus rarely used.

3. Aging hardware and limited maintainability - The system uses discontinued parts, together with a host computer using old software. The system currently also does not work as intended, producing results with poor repeatability. It was therefore difficult to pinpoint the root causes of the errors.

These limitations will later be discussed in Section 3 Design Concepts.

2.3 Displacement Sensors

Displacement measurements are a fundamental aspect of engineering and physics. Determining an object's position or change of position can be vital when concluding results of different testing and within this project the position is needed in order to measure the deformation. The different techniques deployed vary depending on different characteristics such as precision, range and environmental conditions. [9]

With the progression of techniques such as microelectronics, micro-fabrication and nanomanufacturing newer and improved methods are constantly being developed [10]. Although there are a plethora of sensors and methods, to limit the scope this chapter will delve deeper into four different techniques: Linear Variable Differential Transformer (LVDT), Linear encoder, Eddy current and Laser interferometry.

2.3.1 Linear Variable Differential Transformer

LVDT is a contactless sensor capable of measuring sub-micron displacement. It is built up of three solenoid coils wound around a cylindrical tube which generates a magnetic field when current flows through it. This can more easily be observed in Figure 2. It is constructed with a primary coil in the middle with secondary coils on each side. A sinusoidal voltage is applied to the primary coil and in turn induces a voltage on both secondary coils. When the armature moves within the coil the voltage will increase in one secondary coil and decrease in the other. By measuring the voltage differential the change in position of the armature can be determined [1].

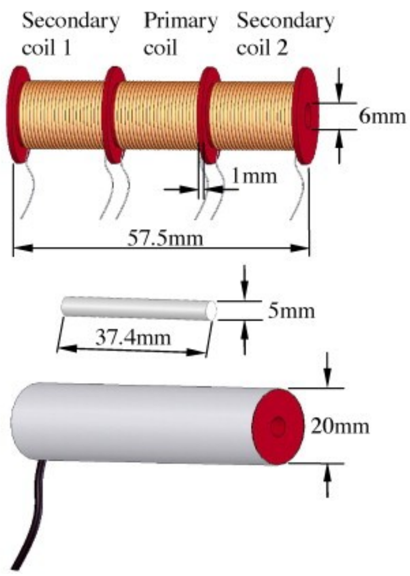

Figure 2: Example of LVDT from top to bottom: Solenoid coils, Armature and Cylindrical tube [1]

The output signal frequency, also known as the excitation frequency, is limited by the supplied frequency range which is specified by the manufacturer with most ranging between 1-10 kHz [11]. A previous implementation of a LVDT was made to measure a ships hull deformation during a voyage proving that this type of sensor is viable within difficult environments and provide reliable displacement data [12].

2.3.2 Linear Encoders

Linear encoders operate by reading a scale (optical, magnetic, inductive, or capacitive) to convert position into electrical signals. They are commonly implemented in industrial applications such as CNC machines because of their high accuracy, resolution, good repeatability and relatively low price [13].

The encoders are capable of measuring in resolutions down to nanometres and incremental encoders allows for sampling frequencies up to several MHz. Some implementations have found success in implementing techniques with linear encoders for resolutions down to 2 nanometres in a range of 50 mm [14].

2.3.3 Eddy Current Sensors

Eddy Current sensors (ECS) work based on electromagnetic induction and can be used to measure displacement in conductive materials without the need of contact. By generating an electrical alternating current in a coil, a magnetic field is generated and when conductive objects approach this coil the field induces circulating currents, so called eddy currents. Based on Lenz's law the currents generate their own opposing magnetic field which interact with the coils magnetic field. The strength of change in impedance is directly correlated to the distance it is thus possible to measure the displacement. Since it is measuring based on magnetic fields it will be unaffected by non-conductive materials.[15]

The excitation frequency of the ECS decides the penetration depth of the eddy currents which is important to keep in mind. However, it is the signal bandwidth which determines the sampling capability, with more high-end ECS boasting several MHz in bandwidth. The resolution of ECS can reach down to the nanometres.[16]

2.3.4 Laser Sensors

Laser sensors is a method utilizing laser and performing measurements based on interference. It is commonly used to measure high-precision characteristics such as displacement, vibrations and surface flatness. Beside the very high precision, they perform non-contact measurements, preserving the properties of the entity being measured. This method is capable of achieving sub-nanometre resolution and bandwidths in the MHz range. However, because of it's high resolution and method of measurement this technique is also sensitive and requires a stable environment [17][18].

2.4 Force and Acceleration Sensors

Stress σ is defined as shown in equation 1, where F is the force, and A is the area. The latter is well defined as the probes area. Simply the circular ending tip of the probe that makes contact with the sample being measured.

The force can be measured directly, using proper sensors, or indirectly using Newton's second law as shown in equation 2 where F is the force, m the mass of the probe, and a is the acceleration that the probe is subjected to. Since the mass of the probe does not vary during measurement and can be quantified, this approach of attaining the force is also valid.

$$\sigma = \frac{F}{A} \tag{1}$$

$$F = ma \tag{2}$$

Therefore, to measure the stress σ, the following sensor solutions were considered:

- Accelerometers;
- Piezo electric force sensors;
- Strain Gauges cells;

2.4.1 Accelerometers

Accelerometers are used to measure acceleration, which can be both static or dynamic. There are multiple different types of accelerometers which include, but are not limited to, resistive, piezoresistive, piezoelectric and capacitive accelerometers.

There is an important distinction between AC and DC accelerometers. AC accelerometers, such as piezoelectric accelerometers, can only measure dynamic acceleration while DC accelerometers, such as resistive, piezoresistive, and capacitive accelerometers, can measure both dynamic acceleration and static acceleration. In our application we are interested in the dynamic acceleration, so both AC and DC accelerometers are suitable. [19]

All mentioned technologies can handle a measurement range of up to 1000's of m/s^2. The other important factors are the resonance frequency and the frequency response. Regarding resonance frequency, the trend is that piezoelectric effect have higher resonance frequencies. What is more critical is the frequency response. In this aspect a clear distinction can be seen between the different sensor technologies. The frequency response of piezoelectric accelerometers can go above 20 kHz, while piezoresistive and resistive accelerometers are generally limited to 5 kHz and the capacitive accelerometer to 1 kHz.[19]

In a similar impact testing machine they made use of the Bruel & Kjaer accelerometer type 4369, a Kistler 5001 charge amplifier and an A/D converter installed in a personal computer and where able to sample the acceleration at 250 kHz. [20]

2.4.2 Piezoelectric Force Sensors

These sensors converts mechanical forces into electric signals using the piezoelectric effect. Applying a force to a piezoelectric crystal results in an output signal in the form of a charge Q, measured in pC. The most commonly used material is quartz, with a sensitivity of $4.3pC/N$ [21]. Their inherent wide frequency response make them suitable for measuring dynamic forces, such as vibrations or impulses. For example, they are used for validating finite-element analysis simulations of impact tests on steel plates, where rapid wave propagation occurs. [22]. The measurement range is typically wide, ranging from as low as $0.1N$ to as high as $60kN$, making these sensors popular across different engineering fields[23] [24]. The linearity error is typically around $\pm0.5\%$ of the full scale output, i.e. a sensor measuring up to $1N$ exhibits a non linearity error of $\pm0.005N$. Applying a preload enhances stability and linearity, especially for ultra small forces.

2.4.3 Strain Gauges Cells

These sensors convert mechanical forces into electric signals leveraging the resistance variation induced by the deformation of a supporting element. The sensitivity of these transducers is quantified through the gauge factor (GF), which represents the magnitude of the electrical resistance variation induced by the deformation. A larger factor means higher sensitivity, thus a small deformation induces a great resistance variation. Silicon-based strain gauges cells have a gauge factor that can go up to 100 [25]. The linearity error is typically around $\pm0.1\%$ of the Full Scale Output. The bandwidth of these transducers can be also wide, up to $100kHz$ making them suitable for sensing high frequency phenomenons like vibrations or impacts [26].

2.5 Thickness Calibration

2.5.1 Standards for Thickness Measurements

The thickness of paper-fiber materials serves as a critical parameter in the measurement process. Due to the presence of voids within the paper-fiber network, which collapse under load, the thickness measured at zero load cannot be regarded as the standard thickness when contact-based measurements are involved. Accordingly, the calibration procedure adheres to the dimensional metrology standards specified by ISO [27] and TAPPI/ANSI [28]. The pressure applied during thickness measurement is standardized at 100 ± 10 kPa.

2.5.2 Electrical-Torque Algorithm

To have the thickness calibration, it's necessary to know the static force on the probe. Considering the stiff connection between the motor and the probe, an effective method is to use an electrical-torque algorithm. Integrating this algorithm with the measurement module is advantageous, as it efficiently reuses precision sensors and actuators.

In rotary electric actuators (e.g., motor), the developed electromagnetic torque is, to first order, proportional to the phase (or armature) current. The essential relation[29] is

$$T_e = K_t i$$

where T_e is the instantaneous electromagnetic torque, i is the measured motor current, and K_t is the torque constant.

The accurate use of the current torque algorithm is based on a well-calibrated K_t and low-latency linear current sensing. Typically, the static force measured by the electrical torque algorithm deviates by about $\pm 5\%$[30]. This level of error remains well within the acceptable tolerance range of 100 ± 10 kPa[27].

2.6 Securing the Sample

There are various methods in use for securing an object in the XY plane, due to different types of material, machines, and intended objectives. In this case, securing thin-layer materials is the concern. To achieve sufficiently high precision, the material has to be securely fixed, thus minimizing potential tolerance errors.

2.6.1 Vacuum Clamping

Vacuum clamping is a method that can be applied to high-precision applications. It can fix the material in position with a uniform distribution of holding force that minimizes both damage and measurement uncertainty from fixation tools [31][32]. This aspect is particularly important for thin or delicate materials.[32]. The working principle consists of holes connected to a vacuum system, which generates negative pressure under the testpiece, allowing it to be held firmly in place [33].

Among the various vacuum generation technologies, the Venturi vacuum generator stands out for its simplicity, reliability, and efficiency as it relies on Bernoulli's principle and

Venturi effect to create a vacuum without requiring mechanical components such as pumps or motors. [34]

2.6.2 Electrostatic Chuck

An electrostatic chuck is a device used for holding workpieces by generating a coulomb force between a workpiece or object and electrodes over which a voltage is applied to achieve adsorption [35][36]. It is applicable over a wide area of workpieces including thin, brittle, or porous work which are difficult to fix without leaving defection using conventional chucks [36].

2.6.3 Adhesive Fixation

An adhesive fixation is a method utilizing adhesives such as tape or glue to bond objects without clamping tools resulting in low stress application and uniform contact [37][38]. The use of adhesive fixation also minimizes the vibrations induced by the tool in the workpiece and minimizes chatter and it is currently used in most cases for fixing complex or low-rigidity parts. [38]

2.6.4 Mechanical Clamping

Mechanical clamping is a method that typically uses a physical clamping tool, for example grips or screws, to secure at the edges of a material. It locks the object in alignment with the direction of the applied load, preventing slippage and ensuring it remains still while proceeding with operations [39][40]. This method is traditional and robust, however, it can cause damage to fragile materials.

2.7 Sampling

Sensors typically output data in the form of analog signals, such as voltage. However, personal computers or microcontrollers are either limited in their ability to process analog signals with high precision or are designed to accept only digital inputs. Therefore, additional hardware is required to perform signal sampling. To ensure accurate reconstruction of the original signal and to prevent aliasing, the Nyquist theorem must be applied during the sampling process[41]. Data Acquisition (DAQ) systems and custom solutions are discussed for sampling.

2.7.1 DAQ

Data acquisition systems, sometimes called data loggers, combine physical hardware and the software necessary to sample signals and interface with computer systems. Applications of DAQ systems include scientific research, industrial automation, environmental monitoring, ect. The key factors defining the performance of DAQ systems are their resolution, sampling rate, and channel count.

An example of a DAQ system is the M4i.4421-x8, from spectrum instrumentation, which can sample at 16 bits on four different channels simultaneously at 180 MS/s. [42]

2.7.2 Custom Solutions

In both industrial applications and everyday use, two types of chips are most commonly employed for signal sampling tasks: microcontroller units (MCUs) and field-programmable gate arrays (FPGAs). In this section, custom solutions based on these two types of chips are discussed.

Modern MCUs are typically equipped with various integrated peripherals, including ADCs. A representative example is the STM32 series, particularly the high-performance STM32H7[43], which can achieve a sampling rate of up to 3.6 Msps at 16-bit resolution. For applications requiring higher precision, external ADC chips such as the ADS1115[44] can be interfaced with the MCU via SPI or I2C protocols. However, MCUs generally exhibit limited noise immunity, have difficulty achieving synchronized signal acquisition, and are constrained by bus bandwidth. As a result, they are more suitable for low-speed sampling applications.

FPGAs are reconfigurable logic devices that support repeated programming via hardware description languages (HDLs), enabling parallel processing capabilities. They are widely employed in systems requiring high real-time performance, such as in telecommunications, industrial automation, and aerospace applications. For instance, the AMD Zynq RFSoC series[45] integrates eight channels of 12-bit, 4.096 Gsps RF-ADCs directly on-chip, enabling ultra-high-speed sampling. The integration of external high-precision ADCs can further enhance sampling accuracy. Nevertheless, FPGAs come with certain drawbacks, including high chip cost, complex development and debugging processes, and stringent requirements for PCB design.

3 Design Concept

In this section the concept for the measurement- and clamping module that will be built and implemented next autumn will be introduced.

3.1 General Concept

Three concepts were generated for the new machine, as can be seen in figure 3. All the concepts generated make use of a linear actuator to lift and drop a probe to generate the impulse, in the same manner as the previous machine, as discussed in section 2.2. What differs from the old product is the addition of new sensors to measure the displacement and the stress.

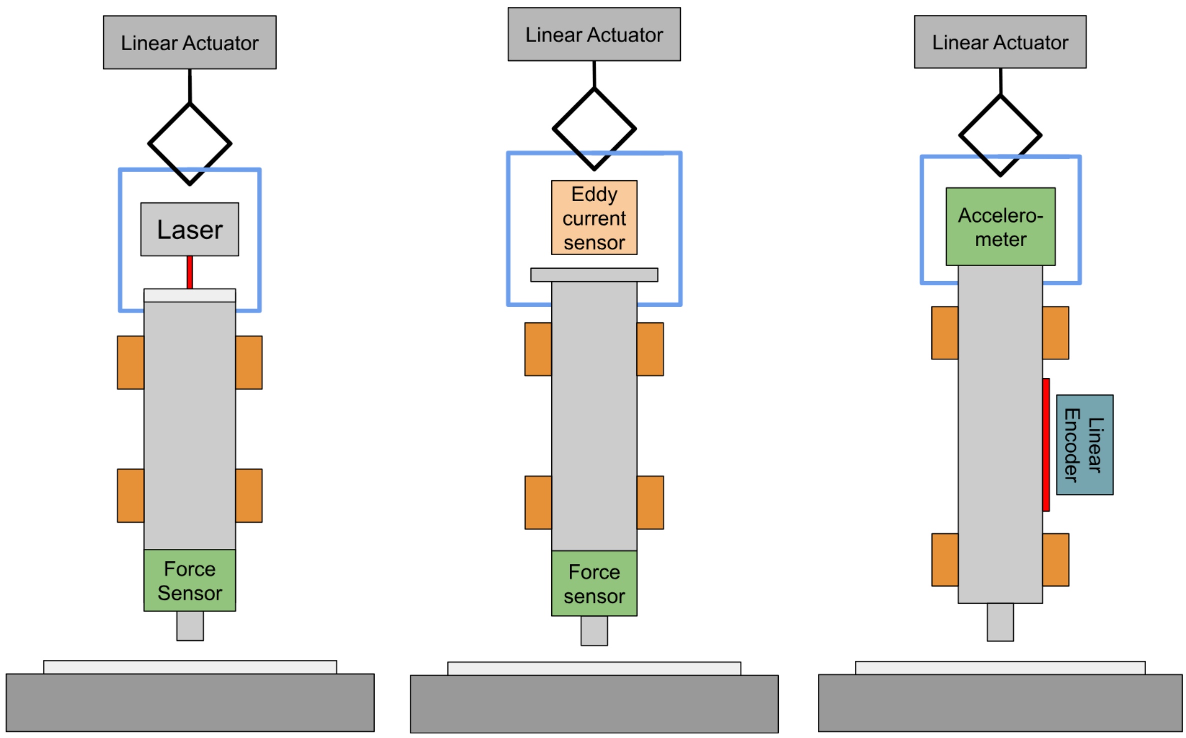

(a) Concept 1 (b) Concept 2 (c) Concept 3

Figure 3: Three concepts for the new machine

Searching for commercially available sensors, that could met the technical requirements for resolution, noise, sampling, and cost, different parts of the concepts showed above were combined: the force sensor showed in figure 3a and 3b, as well as the linear encoder in figure 3c, have been chosen, which resulted in the system that can be seen in figure 4.

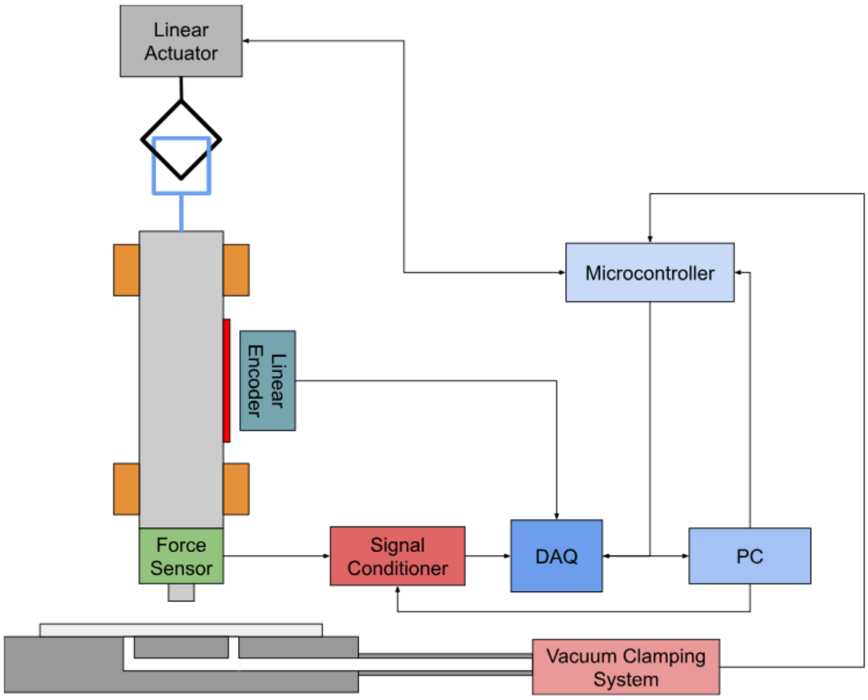

Figure 4: The final concept of the system

For the measurement of the stress, a piezoelectric force sensor was chosen. Although a piezoelectric accelerometer would probably also have worked, there were concerns about the mounting of the sensor and the mass of the probe changing. The mounting of the accelerometer, as shown in figure 3c, would have been on the top of the probe which could potentially distort the signal. Also, since a cable is attached to the sensor mounted on the probe the mass of the probe could vary if the cable shifts. Therefore, a piezoelectric force sensor mounted directly at the point of interest was chosen to be able to neglect the mass and minimize the effects on the signal from the mechanical structure of the machine.

For the measurement of the displacement, a linear encoder was chosen. A laser system and an eddy-current sensor were considered as shown in figure 3a and 3b. Unfortunately the laser system that was found could not sample fast enough and the eddy-current sensor was both out of budget and needed a target that exceeded the diameter probe for the new measuring range. Both these systems would have to be mounted on the top of the probe leading to a potential distortion of the signal. Therefore, the linear encoder was seen as the best option since the measurement happens as close as possible to the point of interest, introduces no friction, allows for a high sampling rate and excellent resolution.

3.2 Implementation of sensor system

The linear encoder that was chosen is the ID1102L from POSIC. This linear encoder is contained in a small package and outputs two A and B signals using quadrature encoding. With an A/B frequency of 1 MHz and a resolution of down to 20 nm. The force sensor chosen was the 208C01 from PCB Piezotronics. This force sensor has a measurement range of up to 44.5 N, a broadband resolution of 0.45 $mN - rms$, and an upper frequency limit of 36 kHz.

The signal from the linear encoder is digital, and the signal from the force sensor is analog. To sample the data from both sensors, a DAQ will be used as shown in figure 4. The 5442D from Pico Technology was chosen as the DAQ system. It has 4 channels; one is used by the force sensor and two by the linear encoder. The DAQ can sample at 125 MS/s in 14 bit mode for three channels simultaneously. The analog signal from the force sensor must first pass through the TA487 IEPE signal conditioner, also from Pico Technology, before interfacing with the DAQ system. The reason for using the same DAQ system for both sensors is to aid in the synchronization of the signals in the time domain.

The DAQ system can be triggered to start recording data from an external input that will be controlled by a microcontroller. After a pre-programmed amount of time, the data will be exported as a file to the PC for further processing.

The linear actuator will also be controlled by the same microcontroller that controls the DAQ system. Therefore, synchronization between dropping the probe and capturing the data can be guaranteed.

3.3 Impulse Generation

As the previous machine performed adequately regarding the fundamental dynamics of the probe, it was concluded that an impulse generation of the same principle as the old machine could be used. As in, a linear actuator moving the probe to the required height and dropping it in free fall to induce the impulse.

This allows the machine to vary the applied force coupled with velocity to the required values. In addition the decoupling system of the previous machine was also chosen as to not include any actuator dynamics.

The acceleration can easily be achieved by linear actuation but the primary benefit from this is that the impact is not affected by anything but the probe, thus allowing the impact dynamics to be dependent only on the probe and test piece.

3.4 Vacuum Clamping System

According to the requirement from the section 1.6, table 1 "Test material shall be secured and not damaged", as well as the limitation point 2. mentioning the clamping functionality, the paper clamping method that appears to be the most suitable solution is a vacuum clamping as it is not only appropriate for high accuracy application, but also it causes minimal risk of mechanical stress from fixation tools which could affect our measurement.

The concept of implementing a vacuum clamping system involves several key components which consists of an air compressor, a solenoid valve, a Venturi vacuum generator, a working surface, including a microcontroller and a silencer. These components are intended to be connected using hoses or tubes and installed beneath the measurement system, as illustrated in figure 4.

The combination of each component and the airflow within the system are shown in the following diagram:

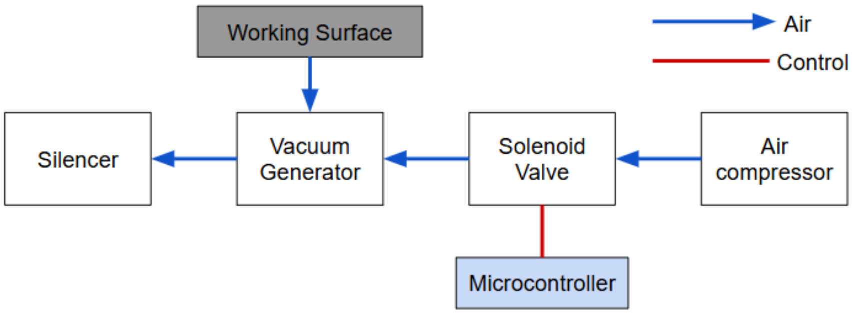

Figure 5: The concept diagram of a vacuum clamping system

As seen in figure 5, the air compressor, the primary source of compressed air, is connected to a solenoid valve that regulates the airflow directed to the Venturi vacuum generator. This valve will be controlled by a microcontroller, which enables the system to be turned on and off automatically.

The Venturi vacuum generator is then connected to the working surface, which characterizes a numerous perforated channels across the surface in order to distribute the holding force. This surface serves as a platform for placing and securing the test material firmly in place and allows atmospheric air to enter the system when the vacuum is activated. Additionally, the silencer can also be installed at the exhaust port to reduce noise from the escaping air.

4 Discussion

In this section the following project work will be discussed which includes future work and potential risks that could arise.

4.1 Challenges for the Autumn Semester

The required machine specifications have been investigated thoroughly but the work has stayed highly theoretical, suppliers have been contacted but the concrete design of the system has not been investigated as rigorously. Some key risks of the project is thus that the implementation of the new system will work with the old and that the lead times for the required changed parts will be within the span of the project as well as that there are no significant oversights to the mechanical principle.

The implementation of a system with multiple high precision sensors is anything but trivial as the sensors have to be timed and calibrated to perform reliable measurements, without this the machine will produce unreliable data even if sensors that can measure within the requirements are used.

In parallel to the sensory and mechanical aspect of the project, the requirements will have to be questioned further as without properly set requirements, the machine might not perform sufficiently even if all requirements are met.

4.2 Future Work

For the coming autumn semester the focus has been set on developing and testing the concept design discussed in section 3. The future work has been divided up into two phases as can be seen in Appendix A. The first phase will be a developing phase with focus on constructing and integrating the components. The second phase will be focusing on validating and verifying the design to ensure it handles all requirements mentioned in 1.6. During this phase the report will also be completed. A preliminary budget has been set and will be reviewed in parallel during the development phase. The GANTT schedule will be reviewed every week by the group to detect trailing tasks and ensure everyone has tasks assigned. Before summer the linear encoder, linear actuator and force sensor will be purchased to ensure they will arrive before the start of phase 2.

References

[1] S.-T. Wu, S.-C. Mo, and B.-S. Wu, "An lvdt-based self-actuating displacement transducer," *Sensors and Actuators A: Physical*, vol. 141, no. 2, pp. 558–564, 2008.

[2] S. Escursell, P. Llorach-Massana, and M. B. Roncero, "Sustainability in e-commerce packaging: A review," *Journal of Cleaner Production*, vol. 280, p. 124314, 2021.

[3] G. K. Deshwal, N. R. Panjagari, and T. Alam, "An overview of paper and paper based food packaging materials: health safety and environmental concerns," *Journal of Food Science and Technology*, vol. 56, no. 10, p. 4391 – 4403, 2019. Cited by: 234; All Open Access, Bronze Open Access, Green Open Access.

[4] Packaging Impressions, "Benchmarking worldwide market trends in flexographic printing," January 2024. Accessed: 2025-05-15.

[5] J. Johnson, *Aspects of Flexographic Print Quality and Relationship to Some Printing Parameters*. Dissertation, Karlstad University, Faculty of Technology and Science, Chemical Engineering, Karlstad, Sweden, 2008. Accessed: 2025-05-15.

[6] Y. Liu, J. H. Y. Lo, J. K. Nunes, H. A. Stone, and H. C. Shum, "High-throughput measurement of elastic moduli of microfibers by rope coiling," *Proceedings of the National Academy of Sciences*, vol. 121, Mar. 2024.

[7] Research Institutes of Sweden (RISE), "About rise." `https://www.ri.se/en/about-rise`, n.d. Accessed: 2025-05-20.

[8] C. Rydefalk, A. Hagman, L. Yang, and A. Kulachenko, "Mechanical response of paperboard in rapid compression – the rapid zd-tester, a measurement technique," 08 2022.

[9] W. Gao, S. Kim, H. Bosse, H. Haitjema, Y. Chen, X. Lu, W. Knapp, A. Weckenmann, W. Estler, and H. Kunzmann, "Measurement technologies for precision positioning," *CIRP Annals*, vol. 64, no. 2, pp. 773–796, 2015.

[10] H. Yu, X. Chen, C. Liu, G. Cai, and W. Wang, "A survey on the grating based optical position encoder," *Optics Laser Technology*, vol. 143, p. 107352, 2021.

[11] Trans-Tek, "Choosing the correct lvdt frequency for your application." `https://transtekinc.com/blog/choosing-the-correct-lvdt-frequency-for-your-application/?utm_source`. Accessed: 2025-05-15.

[12] D. Wang and C. Hao, "Hull deformation measurement equipment based on lvdt sensor," in *2022 IEEE 6th Advanced Information Technology, Electronic and Automation Control Conference (IAEAC)*, pp. 1494–1497, 2022.

[13] D. Gurauskis, K. Przystupa, A. Kilikevičius, M. Skowron, M. Jonas, J. Michałowska, and K. Kilikevičienė, "Performance analysis of an experimental linear encoder's reading head under different mounting and dynamic conditions," *Energies*, vol. 15, no. 16, 2022.

[14] X. Wang, W. Jiang, F. Zhao, Y. Fang, Z. Zhang, X. Ren, L. Yin, Y. Shi, B. Chen, and H. Liu, "A novel peak positioning method for nanometer displacement measurement by optical linear encoder," *Measurement*, vol. 242, p. 115888, 2025.

[15] H. Wang, B. Ju, W. Li, and Z. Feng, "Ultrastable eddy current displacement sensor working in harsh temperature environments with comprehensive self-temperature compensation," *Sensors and Actuators A: Physical*, vol. 211, pp. 98–104, 2014.

[16] B. George, Z. Tan, and S. Nihtianov, "Advances in capacitive, eddy current, and magnetic displacement sensors and corresponding interfaces," *IEEE Transactions on Industrial Electronics*, vol. 64, no. 12, pp. 9595–9607, 2017.

[17] G. Ye, T. Yuan, Y. Zhang, T. Wang, and X. Zhang, "Recent progress on laser interferometry based on vortex beams: Status, challenges, and perspectives," *Optics and Lasers in Engineering*, vol. 172, p. 107871, 2024.

[18] K. Wang, G. Xing, P. Yang, M. Wang, Z. Wang, and Q. Tian, "High-bandwidth heterodyne laser interferometer for the measurement of high-intensity focused ultrasound pressure," *Micromachines*, vol. 14, no. 12, 2023.

[19] S. Elies and S. Ebenhöch, "Performance analysis of commercial accelerometers of different technologies," 2015.

[20] Y. Xu and B. Mellor, "Comparative study of impact and static indentation tests on particulate-filled thermoplastic fluoropolymer coatings," *Proceedings of the Institution of Mechanical Engineers, Part C*, vol. 228, no. 1, pp. 22–30, 2014.

[21] HBKWorld, "Piezoelectric sensors: Which one for my application?."

[22] J. Liu, C. Hei, M. Luo, D. Yang, C. Sun, and A. Feng, "A study on impact force detection method based on piezoelectric sensing," *Sensors*, vol. 22, no. 14, 2022.

[23] GlobalSpec, "Piezoelectric sensor information." https://www.globalspec.com/learnmore/electrical_electronic_components/passive_electronic_components/piezoelectric_devices/piezoelectric_sensors.

[24] GlobalSpec, "Piezoelectric sensor information." https://www.globalspec.com/learnmore/electrical_electronic_components/passive_electronic_components/piezoelectric_devices/piezoelectric_sensors.

[25] Y. S. Taemin Kim, "Ultrathin crystalline-silicon-based strain gauges with deep learning algorithms for silent speech interfaces," *Nature Communications*, vol. 13, 2022.

[26] T. L. Paez, "Harris' shock and vibration handbook."

[27] "Iso 534:2011 paper and board — determination of thickness, density and specific volume," Standard ISO 534:2011, International Organization for Standardization, Geneva, Switzerland, 2011. Accessed: 2025-05-15.

[28] ADMET, "Technical association of the pulp and paper industry, tappi t 411 om-21 – thickness (caliper) of paper, paperboard, and combined board." https://www.tappi.org/product_pull/09/dec/__03/thickness-caliper-of-paper-paperboard-and-combined-board-test-method-t-411-om-15. Accessed: 2025-05-15.

[29] A. Hughes and B. Drury, *Electric motors and drives: fundamentals, types and applications*. Newnes, 2019.

[30] maxon motor ag, "Motor data and operating ranges of maxon dc motors," 2010.

[31] K. Uesugi, F. Shima, K. Fukumoto, A. Hiura, Y. Tsukamoto, S. Miyagawa, Y. Sawa, T. Akagi, M. Akashi, and K. Morishima, "Micro vacuum chuck and tensile test system for bio-mechanical evaluation of 3d tissue constructed of human induced pluripotent stem cell-derived cardiomyocytes (hips-cm)," *Micromachines*, vol. 10, no. 7, 2019.

[32] N. A. Wahab, N. Adlin, M. A. A. Nassiruddin, M. Y. Yaakob, M. H. A. Bakar, M. A. M. Sani, and I. U. Rahman, "Impact of vacuum clamping system designs on surface quality during the end milling process," *MALAYSIAN JOURNAL OF MICROSCOPY*, vol. 20, no. 2, 2024.

[33] VacuumChuck, "How does a vacuum chuck work?." `https://www.vacuumchuck.com/how-a-vacuum-chuck-works/`, 2011. Accessed: 2025-05-15.

[34] N. Kroupa, "The science behind venturi vacuum generators: How they create suction without moving parts." `https://vac-cube.com/blog/post/the-science-behind-venturi-vacuum-generators-how-they-create-suction-without-movi` 2025. Accessed: 2025-05-19.

[35] S. B. Kim, J. H. Kim, and D. K. Min, "Study of chucking force distribution according to substrate pattern and deformation characteristics of electrostatic chuck for deposition," *Journal of Electrostatics*, vol. 133, p. 104008, 2025.

[36] T. S. C. Ltd, "About electrostatic chucks." `https://tsukubaseiko.co.jp/english/feature/chucks-overview.html`. Accessed: 2025-05-15.

[37] ABB, "Lw zd tensile tester." `https://library.e.abb.com/public/c1bd4260145249ab8e55a7786ef6f775/285_LW_ZD_Tensile_Tester_v2.0.pdf`, 2017. Accessed: 2025-05-15.

[38] N. A. Panc, V. Bocaneț, C. Vilău, H. Chezan, I. A. Popan, and G. Conțiu, "New method of fixturing the low-rigidity parts by adhesive clamping," *The International Journal of Advanced Manufacturing Technology*, vol. 129, no. 5, pp. 2591–2608, 2023.

[39] J. Orellana Barrasa, A. Ferrández-Montero, B. Ferrari, and J. Y. Pastor, "Characterisation and modelling of pla filaments and evolution with time," *Polymers*, vol. 13, no. 17, 2021.

[40] ADMET, "Tappi t456 water-saturated paper and paperboard tensile testing." `https://www.admet.com/testing-applications/testing-standards/tappi-t456-water-saturated-paper-paperboard-tensile-testing/`. Accessed: 2025-05-15.

[41] A. V. Oppenheim, A. S. Willsky, and S. H. Nawab, *Signals and systems*. Pearson Education, 1997.

[42] S. Instrumentation, *M4i.44xx-x8 - 14/16 bit Digitizer up to 500 MS/s*.

[43] STMicroelectronics, *RM0433 Reference manual*, 2023. Reference Manual RM0433, Rev. 8.

[44] Texas Instruments, *ADS111x Ultra-Small, Low-Power, I2C-Compatible, 860SPS, 16-Bit ADCs with Internal Reference, Oscillator, and Programmable Comparator*, 2024. Datasheet, SLAS990N, DEC 2024.

[45] AMD Xilinx, *Zynq UltraScale+ RFSoC: Technical Reference Manual*, 2025. UG1085 (v2.5).

A Autumn Plan

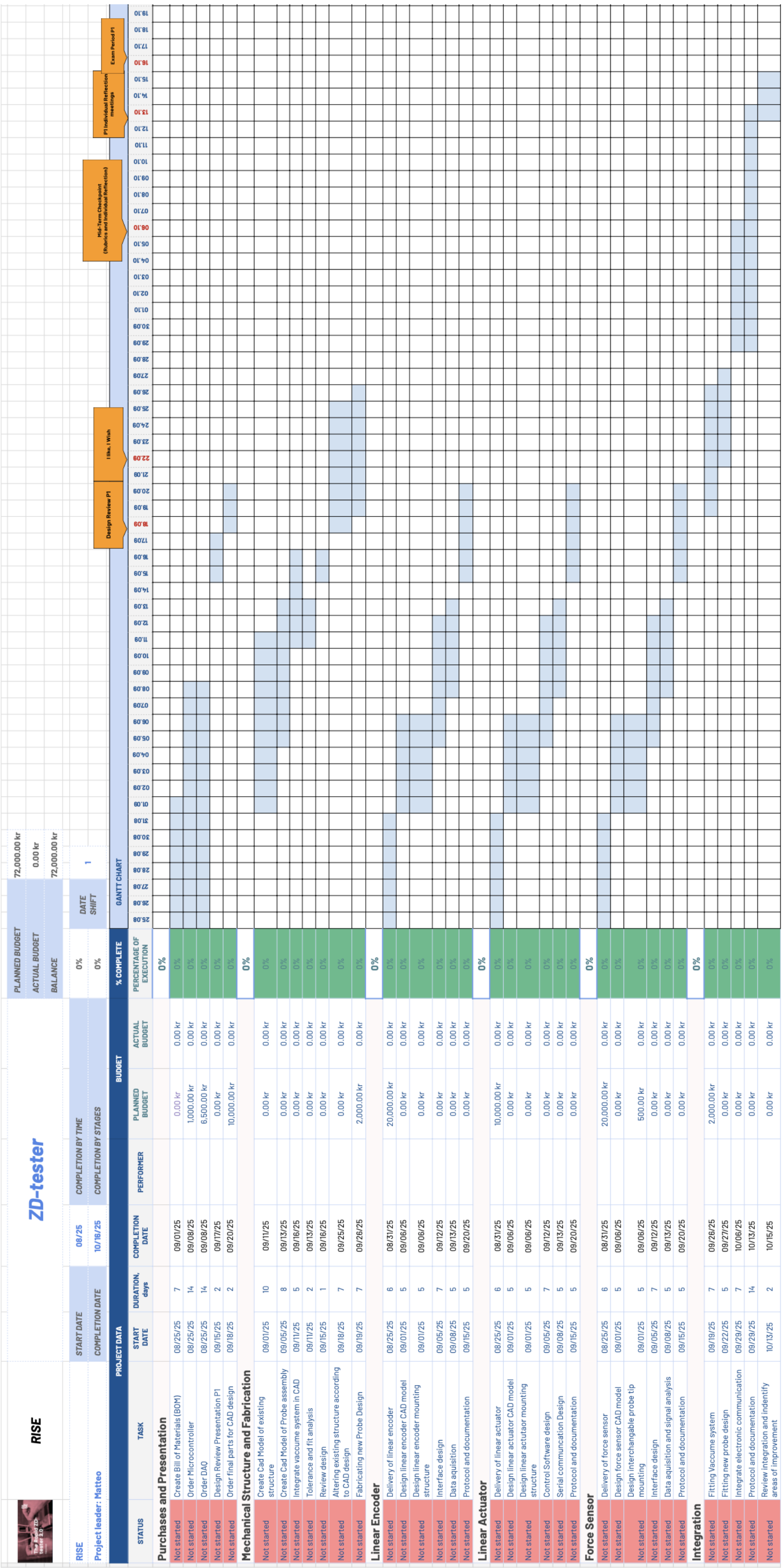

Figure 6: GANTT Chart for Phase 2

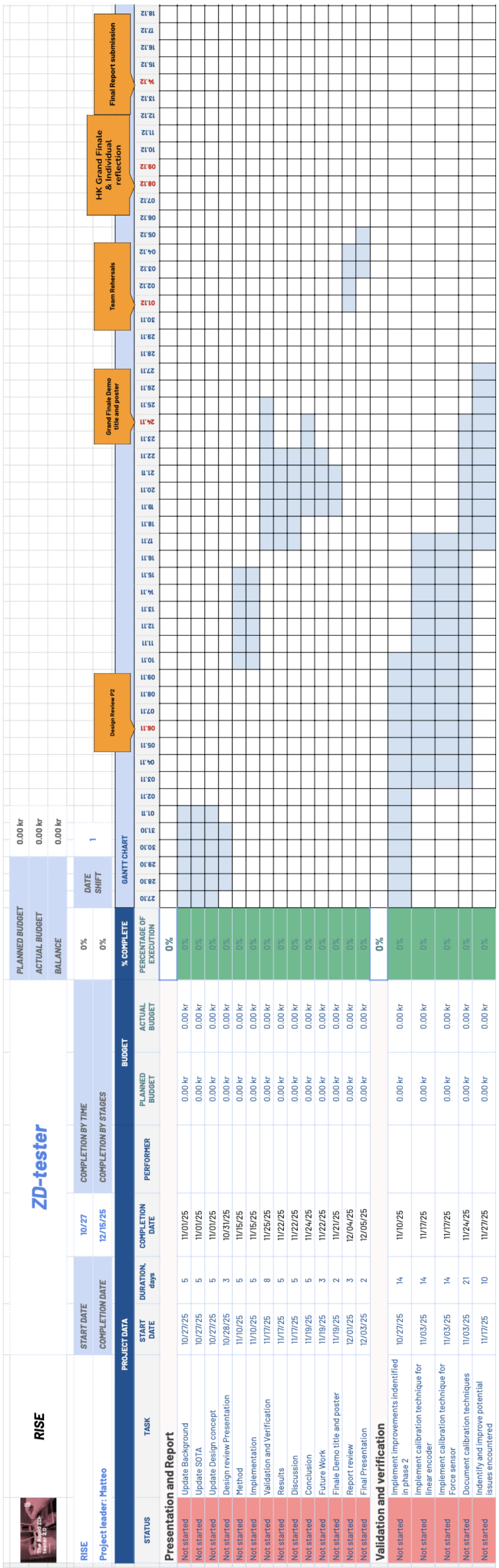

Figure 7: GANTT Chart for Phase 3

B Risk Assessment

Arbetsmiljö

Aktivitet: Blankett för riskbedömning och handlingsplan				
Dokumentet framtaget av: Carl Bermhed	Dokumentdatum: 2024-04-28	Skyddsombud (sign.):	Version: 1	Sida: 1 (1)

Riskbedömningen omfattar följande plats/platser:	Datum:	Riskbedömningen genomförd av:
Kurs: MF2121. Team: **RISE** Plats : *Cave*	2025.05.	Micke Hellgren / Daniel Frede
Ansvarig chef har tagit del av nedan (signatur och datum)		

Resultat av riskbedömning			Handlingsplan			
Riskkällor och risker	**Allvarlig risk**	**Annan risk**	**Åtgärder**	**Ansvarig**	**Klart när?**	**Uppföljning/ kontroll**
The machine is mounted on a heavy stone slab which might be dropped during transport		Medium	Make sure to use proper moving equipment for transporting it.			
The stone slab might cause the table to collapse causing injury		Low	Make sure that a rigid table is used for the slab.			

Mechatronics Division, KTH Department of Engineering Design

Figure 8: Risk Assessment Report (RISE)